GROUND MOVEMENTS DUE TO SHALLOW TUNNELS IN SOFT GROUND: 2. ANALYTICAL INTERPRETATION AND PREDICTION

by

Federico Pinto[1], Despina M. Zymnis[2] and Andrew J. Whittle[2]

ABSTRACT: This paper considers the practical application of analytical solutions for estimating ground movements caused by shallow tunneling in soft ground using closed-form expressions presented in a companion paper based on linearly elastic and average-dilation models of soil behavior (Pinto and Whittle, 2011). The analytical solutions express two dimensional distributions of ground deformations as functions of three parameters: the uniform convergence and relative ovalization of a circular tunnel cavity, and either the Poisson's ratio or the average dilation angle for elastic and plastic behavior, respectively. This paper shows that the analytical predictions can achieve very good representations of the distribution of far field deformations through a series of case studies in clays and sand. In some cases, the input parameters can be interpreted from a simple calibration to three independent measurements of ground displacements comprising surface settlements above the tunnel centerline and at a reference offset, and the lateral displacement at the springline elevation, recorded by an inclinometer at an offset of one tunnel diameter from the centerline. However, it is generally more reliable to use a least squares fitting method to obtain the model input parameters, using all available extensometer and inclinometer data.

KEYWORDS: Tunnel, ground movements, analytical solutions, field performance, elasticity, plasticity

[1] Universidad Nacional de Córdoba, Córdoba, Argentina
[2] Massachusetts Institute of Technology, Cambridge, MA

INTRODUCTION

All methods of tunneling have the potential to produce deformations in the surrounding soil. Figures 1a and 1b illustrate the primary sources of movements for cases of closed-face shield tunneling and open-face sequential support and excavation (often referred to as NATM), respectively. For closed-face shield tunneling (e.g., EPB or slurry support), ground movements due to stress changes around the tunnel face may be less significant than those caused by overcutting or plowing of the shield or ground loss around the tail void. In contrast, the large changes in stresses around the tunnel heading are clearly important factors for tunnels built by sequential excavation and support, and are typically mitigated by local reinforcement or reducing the round length. In either case, the 3D nature and complexity of the sources of ground movement are readily apparent (even without accounting for stratigraphic variations, groundwater conditions etc.).

Current geotechnical practice relies almost exclusively on empirical methods for estimating tunnel-induced ground deformations. Following Peck (1969) and Schmidt (1969), there is extensive experience in characterizing the transverse surface settlement trough using a Gaussian function:

$$u_y(x,y) = u_y^0 \exp\left(\frac{-x^2}{2x_i^2}\right) \qquad (1)$$

where x is the horizontal distance from the tunnel centerline, u_y^0 is the surface settlement above the tunnel centerline, and the location of the inflection point, x_i, defines the trough shape.

Mair and Taylor (1997), show that the width of the surface settlement trough can be well correlated to the tunnel depth, H, and to characteristics of the overlying soil (see Figure 2a). The trough width ratio varies from $x_i/H = 0.35$ for sand to 0.50 for clays. They have also attempted to

extend the same framework for subsurface vertical movements by characterizing the trough width parameter as a function of depth:

$$x_i = K(H - y) \tag{2}$$

This involves significantly more uncertainty and requires an empirical function to define K as shown in Figure 2b. There is also very limited data for estimating the horizontal components of the ground movements. The most commonly used interpretation is to assume that the displacement vectors are directed to the center of the tunnel as proposed by Attewell (1978) and O'Reilly & New (1982) such that:

$$u_x = \left(\frac{x}{H}\right) u_y \tag{3}$$

The companion paper (Pinto & Whittle, 2011) has presented and compared a series of analytical solutions for estimating ground movements around shallow tunnels. These solutions make gross approximations of real soil behavior (either linear elastic or plastic with constant dilation), yet otherwise fulfill the principles of continuum mechanics. The effectiveness of these analytical solutions resides in the fact that the complete field of ground movements (u_x, u_y for the transverse plane) can be described by means of 3 parameters, two of which characterize the modes of tunnel deformation around the tunnel cavity: u_ε, the uniform convergence and ρ (= $-u_\delta/u_\varepsilon$), the relative distortion; and one soil property, either Poisson's ratio, ν, for the elastic case or α, the average dilation for plastic soil deformation (see Figure 3a).

This paper presents a detailed evaluation of the 'approximate', closed-from analytical solutions obtained by superposition of singularity solutions (Pinto & Whittle, 2011) through a series of case studies. Although similar validation studies have been reported elsewhere (e.g., González & Sagaseta, 2001) the goal of this work is to establish the capabilities of the analyses

for representing the distribution of ground movements. The reliability of these predictions is of critical importance in estimating the effects of tunnel-induced ground deformations on adjacent facilities such as pipelines (Vorster et al., 2005) or pile foundations (Kitiyodom et al., 2005). The goal of the paper is to establish the analytical solutions as a credible alternative to existing empirical methods and to show their advantage in computing ground deformations compared to much more demanding non-linear numerical analyses. The current validation is helpful in defining typical ranges of the input parameters for given ground conditions and tunneling method but does not yet provide sufficient data to enable the analyses to be used in predicting tunnel performance.

EVALUATION OF INPUT PARAMETERS

In principle, the input parameters for the analytical solutions can be derived from three independent field measurements. Surface settlements are routinely measured in tunnel projects. However, there is no standardization in the layout of instrumentation for monitoring subsurface movements. Pinto (1999) proposed a procedure that uses the following field measurements with sign convention shown in Figure 3:

1. The vertical displacement at the surface above the centerline of the tunnel; u_y^0.
2. The vertical surface displacement at a reference offset, $x/H = 1$, where H is the depth to the tunnel springline, u_y^1.
3. The horizontal displacement at the elevation of the tunnel springline ($y/H = -1$) measured in a reference inclinometer installed at an offset of one radius from the tunnel wall (i.e., $x/R = 2$), u_x^0.

The surface settlement ratio, u_y^1/u_y^0, is a measure of the trough shape and is highly sensitive to variations in the relative distortion, ρ, and dilation parameter, α, as shown in Figure 4a. Similarly, the horizontal displacements in the reference inclinometer (i.e. the measurement ratio, u_x^0/u_y^0) are also controlled by ν, ρ and α, as illustrated in Figure 4b.

Figure 5a shows that it is possible to define unique values of ρ, ν or α from these two measurement ratios. It is important to note that the linearly elastic and average dilation solutions coincide for the case where $\nu = 0.5$ and $\alpha = 1$, corresponding to undrained shearing associated with short-term ground movements of tunnels constructed in low permeability clays. Finally, the uniform convergence of the tunnel cavity, u_ε, can be obtained by matching the analytical and measured centerline surface displacements, u_y^0, as shown in Figure 5b, from which the ground loss at the tunnel cavity can then be obtained directly, $\Delta V_L/V_0 = -2u_\varepsilon/R$.

An alternative approach to parameter selection is to use a least squares fitting approach to the available vertical and horizontal displacements. Surveys of surface settlements typically involve up to 5-10 offset locations (at a given section), while subsurface movements are usually obtained from measurements in small number of vertical boreholes. These vertical movements using rod or multi-point borehole extensometers, and horizontal displacements (in two orthogonal directions) from tilt measurements using inclinometers. The current least squares fitting method considers each displacement component independently and uses a balanced number of vertical and horizontal measurements, excluding points that are very close to the tunnel, where far field and constitutive approximations in the analytical solutions become significant (Pinto and Whittle, 2011).

The current applications focus on least squares solutions for the tunnel cavity deformations parameters (i.e., u_ε, u_δ or ρ) based on assumed values of the soil properties (ν or α). The square solution error (SS) is defined as:

$$SS = \sum_i \left[\left(\tilde{u}_{xi} - u_{xi} \right)^2 + \left(\tilde{u}_{yi} - u_{yi} \right)^2 \right] \tag{4}$$

where $\left(\tilde{u}_{xi}, \tilde{u}_{yi} \right)$ are the measured displacement components at location, i, and $\left(u_{xi}, u_{yi} \right)$ are the computed values at the same location for given set of the input parameters (u_ε, u_δ).

The input parameters can then be optimized from the global minimum error (Least Squares Solution, LSS), as shown in Figure 6. In most practical cases, engineers will expect to fit the measured centerline surface settlement, $\tilde{u}_y^0$, hence, the preferred approach is to present a modified least squares solution, LSS*, that includes this additional constraint.

CASE STUDIES

Table 1 lists the projects considered in this paper and summarizes the model input parameters used in the analyses.

1. EPB Tunnel in Recent Bay Mud (N-2 contract), San Francisco

The San Francisco Clean Water Project N-2 contract was the first US project to use an EPB shield (3.7m O.D.) to construct a 3.56m diameter tunnel through Recent Bay Mud (Clough et al., 1983; Finno & Clough, 1985). The project included 4 lines of instrumentation to measure subsurface ground displacements, each with 5 inclinometers equipped with telescoping couplings to enable vertical displacements to be measured at 3m intervals.

Figure 7b shows the typical profile at the site (near instrumentation line #4, R/H = 0.19) comprising 6.6m rubble fill underlain by 7.1m of recent Bay Mud, colluvium and residual sandy clay. Clough et al. (1983) report undrained shear strengths of the Recent Bay Mud (from UU triaxial tests) increasing with depth from s_u = 24 - 28kPa, and overload factors ($\gamma H/s_u$) in the range 5-6. Hence, large zones of plasticity can be expected within the soft clay. The authors also reported that the actual tunnel construction used relatively high face pressure near to line #4, ($p/\gamma H$ = 0.8) due to clogging in the screw auger. Figure 7a shows the surface and subsurface settlements measured at line #4, 15 days after the passage of the EPB shield.

The conventional empirical model (eqn. 1) fits the measured surface settlement trough with measured centerline settlement, $\tilde{u}_y^0$ = 30.5mm, and fitted inflection width ratio, x_i/H = 0.42 (hence, the apparent tunnel volume loss $\Delta V_L/V_0 = \sqrt{2/\pi}\left[\left(x_i/R\right)\left(u_y^0/R\right)\right] = 3.1\%$).

The input parameters for the analytical solutions can be obtained by the three-point matching procedure proposed by Pinto (1999). The lateral displacement at the springline can be interpreted from the inclinometer data, $\tilde{u}_x^0$ = 21.1mm. It is important to note that the N-2 tunnel caused outward movements of the ground at this location due to the high face pressure imposed during construction at this section and the low K_0 conditions expected in the recent Bay Mud. This result contradicts conventional empirical assumptions (cf. eqn. 3). The third parameter u_y^1 was not measured directly as there were no surface settlement measurements at offsets, |x/H| > 0.6. However, assuming that undrained conditions prevail and hence, $\nu = 0.5$ (or $\alpha = 1$), unique analytical solutions are obtained with measurement ratios u_x^0/u_y^0 = -0.69 and $u_y^1/u_y^0 = 0.12$, as shown Figure 5a (hence, u_y^1 = 3.5mm) for a relative distortion, ρ = 1.76. Hence, the tunnel

cavity parameters are derived as u_ε = -17.9mm, with an equivalent volume loss, $\Delta V_L/V_0$ = 2.0%, Figure 5b.

Figure 6a shows the more complete evaluation of the analytical input parameters at line #4 using a least squares fitting approach with a total of 5 surface settlement and 23 subsurface horizontal and vertical displacement component measurements (Clough et al., 1983). The results show significant differences between the LSS and constrained LSS* solutions, mainly due to significant asymmetry observed in the field measurements. The measured asymmetry can be attributed in part to variations in stratigraphy that are not considered in the analytical solutions. Input parameters for the LSS* solution, ρ = 2.11 and u_ε = -16mm (with an equivalent volume loss $\Delta V_L/V_0$ = 1.8%) differ only slightly from the simpler 3-point matching procedure.

Figures 7a and b compare the analytical (LSS* and 3-point) solutions with the measured vertical and lateral displacement components. The results show a very reasonable match to the distribution of ground movements around the tunnel, and provide a clear indication of the importance of the ovalization mode (u_δ) in explaining tunnel-induced ground movements and in estimating the volume loss associated with the tunnelling process.

Similar methods of parameter selection have been applied to data from instrumentation line #2 of the N-2 project, where a much lower face pressure was used ($p/\gamma H$ = 0.4). Figure 8 shows that the two independent measurements (u_y^0 = 45.7mm, u_x^0 = -5.3mm; u_x^0/u_y^0 = 0.12) imply a much lower distortion ratio, ρ = 0.43 at this section, and not surprisingly much higher ground loss than at line #4 (u_ε = -64.4mm and $\Delta V_L/V_0$ = 7.2%, Fig. 6b). The least squares fitting analysis considered 20 subsurface displacement measurements and the centreline surface settlement u_y^0 (the surface settlement trough was not surveyed at this section) as shown in Figure 6b. The LSS* solution (ρ = 0.61, u_ε = -56mm and hence $\Delta V_L/V_0$ = 6.3%) is again in reasonable

agreement with the simpler 3-point matching solution and both provide consistent estimates of the distribution of ground movements at line #2 as shown in Figure 8.

2. Sewer tunnel Mexico City

The tunnel considered in this section is part of the sewerage system of the Mexico City Metropolitan area. The excavation was made with a shield and pressurized slurry at the tunnel face. Precast segmental linings were installed and at the same time grouting was used to fill the gap between the ring and tunnel wall (Romo, 1997). Tunneling was undertaken through soft clay deposits, underlying approximately 6m of silt and clay partings as shown in Figure 9b.

The tunnel has a circular cross-section of radius R = 2m and a depth to tunnel springline H = 12.75m (R/H = 0.157). Using the measured ground displacement ratios, $u_x^0 / u_y^0 = -0.41$ and $u_y^1 / u_y^0 = 0.23$, Pinto (1999) obtained 3-point matching parameters u_ε = -22mm ($\Delta V_L/V_0$ = 2.2%), ρ = 1.53 and ν = 0.12. While these parameters produce very reasonable agreement with the subsurface movements as shown in Figure 9, the low value of ν is difficult to justify. In fact, Romo (1997) reports a 1m thick sand seam at the elevation of the springline. Pinto (1999) also found that the parameters are strongly affected by the accuracy of the measured value, u_x^0 (and hence, the accuracy of a single reference inclinometer). The least squares analysis uses 26 displacement components, including laterals displacements from 3 inclinometers and settlements at 3 elevations. The analysis also assumes undrained behavior of the soil (i.e., ν = 0.5) to produce an LSS* solution with input parameters u_ε = -25mm ($\Delta V_L/V_0$ = 2.5%) and ρ = 1.34.

Figure 9a compares the analytically computed and measured settlement troughs at three elevations (y = 0, -5 and -10m) within the overlying clay layer. The model predictions are generally in good agreement with the field measurements except at locations close to the tunnel centerline, where both sets of analytical solutions overestimate the measured settlements. Figure 9b compares the analytically computed and measured lateral displacements at three inclinometer positions (x = -2.5m, 2.5m and 4.5m). It is observed that the analytical solutions successfully capture the distribution of lateral movements caused by slurry-shield tunnel excavation. Surprisingly, the 3-point matching provides better agreement with the measured data than the LSS* solutions.

3. Madrid Metro Extension

Approximately 20% of the extension of the Madrid Metro system (1995-1999) was constructed using sequential open-face excavation (referred to as the 'Belgian method'; Gonzalez and Sagaseta, 2001) within tertiary deposits comprising stiff, overconsolidated clays, covered by quaternary sediments. Figure 10 summarizes the field measurements from a typical section (Line 1, Section 7; Sagaseta and Gonzalez, 1999) that include surface settlements and lateral displacements recorded in a single inclinometer (at x = -8m). The tunnel has a horseshoe-shaped area of 62 m^2 (equivalent circular radius, R_{eq} = 4.44 m), a depth to springline H = 15.2 m and an embedment ratio R/H = 0.29.

The input parameters suggested by the 3-point matching technique correspond to u_ε = -13.5mm ($\Delta V_L/V_0$ = 0.6%), ρ = 0.22 and ν = 0.5, and are similar to values reported independently by Sagaseta and Gonzalez (1999). The LSS* solution using all of the available field measurements produces u_ε = -14mm ($\Delta V_L/V_0$ = 0.6%), ρ = 0.21 and ν = 0.5 and all three

solutions describe very well the measured ground movements. The small values of relative distortion may reflect details of the excavation sequence and the high K_0, strength and stability of the overconsolidated clay.

4. Second Heinenoord Tunnel

The Second (Tweede) Heinenoord tunnel was built in order to relieve the large traffic volumes in the existing Heinenoord Tunnel, which crosses under the river Oude Maas, south of Rotterdam. The Dutch Ministry of Transportation selected the Second Heinenoord Tunnel to be the pilot project for the construction of shield-driven tunnels in the Netherlands, since it was the first time that the shield-tunneling technique was used in the country (van Jaarsveld et al., 1999). The soil stratigraphy at the instrumented site comprises 17m deep Holocene layer that mainly consists of loose to medium sands, overlying an 8m deep layer of dense to very dense sands, followed by 2m of stiff silty clays and dense sands, Figure 11. The average ground water table was 3m below ground level. Construction of the tunnel began in 1996 and was completed in June 1997. The tunnel consisted of twin tubes, each with a radius R = 4.15m, depth to springline, H = 16.65m (R/H = 0.25). Tunnel-induced ground movements were extensively monitored with numerous surface settlement markers, 6 extensometers that measured subsurface settlements at 6 elevations and 4 inclinometers that measured horizontal displacements at the locations shown in Figure 11.

Since the tunnel was constructed in sand, it is expected that volume changes will take place due to drained shearing within the soil mass and hence, the most appropriate framework,

are the analytical solutions for a plastic, dilating soil. However, the measurement ratios $u_x^0/u_y^0 = 0.07$ and $u_y^1/u_y^0 = 0.04$ at this site fall outside the range of behavior expected from the 3-point design charts (cf., Fig. 5a with R/H = 0.25). A least squares solution was obtained using the displacement component data shown in Figure 11 generating an LSS* solution with u_ε = -26mm ($\Delta V_L/V_0$ = 1.3%), ρ = 0.80 and α = 1.09. These analyses describe very well the distribution of vertical displacements throughout the soil mass. The results for the lateral displacements are also in good agreement with the measured data except at locations within the inclinometer nearest to the tunnel and at two elevations close to the springline. Figure 11 shows that when these two near-field points are excluded from the LSS analysis, the plastic (average dilation) solution gives remarkably good predictions of the ground deformation field for the second Heinenoord tunnel.

5. Heathrow Express Trial Tunnel

The Heathrow Express (HEX) trial tunnel was built in 1992, in order to examine local ground response to three different sequential construction procedures using the New Austrian Tunneling Method (NATM) in London Clay, each over a length of 30m (Deane and Bassett, 1995). The current analyses focus on the 'Type 3' sequence, which comprised a top heading and bench sequence, with the bottom of the heading supported on inverted shotcrete arches to limit excess settlement. Ground movements are analyzed for the end of the construction phase (May 29, 1992). The local stratigraphy comprised 1-2m of made ground and 2-4m of dense terrace gravels overlying a deep layer of stiff, heavily overconsolidated London Clay (more than 45m thick). The trial tunnel was excavated entirely within the London Clay, as shown in Figure 12. The ground movements induced by the excavation of the tunnel were measured from a virtually

greenfield site, with no significant structures in the zone of influence and the instrumentation used to measure the ground movements included leveling pins for surface movements and 4 inclinometers for subsurface horizontal movements. The key geometric parameters of the tunnel are depth to springline, H = 19m, and equivalent circular radius, R = 4.25m (R/H = 0.22).

The 3-point parameter selection technique cannot be directly applied for this case as the measured ratios $u_x^0/u_y^0 = 0.36$ and $u_y^1/u_y^0 = 0.10$ are outside the bounds expected from the analytical solutions (cf., Fig. 5a with R/H = 0.22). Figure 12 illustrates the dilemma for this case study. By assuming incompressibility of the soil ($\nu = 0.5$) and matching two measurements (u_y^0 and u_x^0) the analytical solutions achieve excellent agreement with the distribution of horizontal displacements as shown in Figure 12b. However, the analyses predict a much wider settlement trough than is found in the measurements (Fig. 12a). The least squares approach uses all of the available displacement component data (excluding potentially misleading near field points close to the tunnel cavity). The corresponding LSS* solution achieves a modest improvement in the computed settlement trough shape (Fig. 12a) but matches only the shallow subsurface horizontal movements (for depths up to 10m). The Authors have made a very detailed assessment of this problem. The observed ground response, characterized by a narrow settlement trough and lateral displacements directed towards the tunnel can be explained by the strong anisotropy in stiffness properties of the London Clay. This has been investigated further through the extension of the analytical solutions to incorporate cross-anisotropic elastic stiffness properties (Zymnis et al., 2011).

CONCLUSIONS

Analytical predictions of far-field ground deformations (Pinto & Whittle, 2011) have been compared to in-situ measurements for construction of five tunnels excavated through different soils and using a variety of construction methods. The paper has compared two different methods for selecting input parameters using 1) three-point matching and 2) least squares fitting method. The three-point method relies on measurements of the trough width $\left(u_y^1\right)$ and lateral displacements at a reference springline location $\left(u_x^0\right)$. When these are available and reliable, there is a very good matching with the least squares solution. However, the Least Squares technique appears less prone to error and has been used successfully on all of the reported case studies. The case studies presented in the paper include tunnels excavated by mechanical boring machines (EPB, slurry shield) and sequential construction (NATM, Belgian method) in a variety of ground conditions. Volume losses $\left(\Delta V_L/V_0 = -2u_\varepsilon/R\right)$ inferred from the data range from 0.6-7.2% with relative distortions $\rho\left(=-u_\delta/u_\varepsilon\right)=0.20-2.11$. The lowest volume loss and distortion parameters were obtained for open face excavation of the Madrid Metro extension project, in very stiff overconsolidated clay. The highest volume losses and distortions were from EPB construction of the N2 tunnel in soft Bay mud. In this case the control of face pressure is the key parameter controlling ground movements. Significant ovalization in this case also relates to the low K_0 value in the soft Bay mud. The analytical solutions describe very well the distributions of ground movements in four of the five cases presented, but appear to overestimate the width of the settlement trough for the NATM construction of the Heathrow Express Trial tunnel. This behavior is attributed to anisotropic stiffness parameters that are considered elsewhere (Zymnis et al., 2011). The paper shows that the proposed analytical solutions represent a very attractive framework for estimating far-field

ground displacements induced by tunnels when compared to purely empirical solutions or to more complex non-linear numerical analyses.

ACKNOWLEDGMENTS

The original research (FP) on this topic was supported by a grant from GMAEC, Tren Urbano in San Juan, Puerto Rico. The second Author (DMZ) also gratefully acknowledges support from the George and Maria Vergottis and Goldberg-Zoino fellowships for supporting her graduate studies at MIT.

REFERENCES

Attewell, P. B. (1978); "Ground movements caused by tunnelling in soil," *Proc. Int. Conf. on Large movements and Structures (ed. J. D. Geddes),* Pentech Press, London, 812-948.

Clough, G. W., Sweeney, B. P., and Finno, R. J. (1983); "Measured soil response to EPB shield tunneling," *Journal of Geotechnical Engineering*, Vol. 109, No. 2, pp. 131-149.

Deane, A. P., and Bassett, R. H. (1995); "The Heathrow Express Trial Tunnel". *Proc. Instn. of Civ. Engrs, Geotech. Engng*., 113, 144-156.

Finno, R. J. (1983); "Response of cohesive soil to advanced shield tunneling," *Ph.D. Thesis*, Stanford University, Stanford, CA.

Finno, R. J., and Clough, G. W. (1985); "Evaluation of soil response to EPB shield tunneling," *Journal of Geotechnical Engineering*, Vol. 111, No. 2, 155-173.

González, C., and Sagaseta, C. (2001); "Patterns of soil deformations around tunnels. Application to the extension of Madrid Metro," *Computers and Geotechnics*, 28, 445–468.

van Jaarsveld, E. P., Plekkenpol, J. W., and Messemaeckers van de Graaf, C. A. (1999); "Ground deformations due to the boring of the Second Heinenoord Tunnel," *Geotechnical Engineering for Transportation Infrastructure*, Barends et al. (eds), Balkema, Rotterdam

Kitiyodom, P., Matsumoto, T., and Kawaguchi, K. (2005); "A simplified analysis method for piled raft foundations subjected to ground movements induced by tunneling,"

International Journal for Numerical and Analytical Methods in Geomechanics, Vol. 29, No. 15, 1485-1507.

Mair, R. J., and Taylor, R. N. (1997); "Bored Tunneling in the Urban Environment", *Proceedings of the 14th International Conference on Soil Mechanics and Foundation Engineering,* Hamburg, pp. 2353–2385.

Möller, S. (2006); "Tunnel induced settlements and structural forces in linings," Ph.D. Thesis, Institut für Geotechnik, Universität Stuttgart

O'Reilly, M. P., and New, B. M. (1982); "Settlements above tunnels in United Kingdom—their magnitude and prediction". *Tunnelling 82*, London, IMM, 173–181.

Peck, R. B. (1969); "Deep Excavations and Tunnels in Soft Ground". *Proceedings of the 7th International Conference on Soil Mechanics and Foundation Engineering*, Mexico City, State of the Art Volume, pp. 225-290.

Pinto, F. (1999); "Analytical Methods to Interpret Ground Deformations due to Soft Ground Tunneling," *S.M. Thesis*, Dept. of Civil and Environmental Engineering, MIT, Cambridge, MA.

Pinto, F., and Whittle, A. J. (2011); "Ground Movements due to shallow tunnels in soft ground: 1. Analytical solutions," Submitted for publication ASCE Journal of Engineering Mechanics, 2011.

Romo, M. P. (1997); "Soil Movements Induced by Slurry Shield Tunneling". *Proceedings of the 14th International Conference on Soil Mechanics and Foundation Engineering*, Hamburg, 3, pp. 1473-1481.

Sagaseta, C., and González, C. (1999); " Capítulo 6.2. Predicción teórica de subsidencias," Aspectos Geotécnicos de la Ampliación del Metro de Madrid, Communidad de Madrid (In Spanish).

Schmidt, B. (1969); "Settlements and ground movements associated with tunneling in soils," *PhD Thesis*, University of Illinois, Urbana.

Vorster, T. E. B., Klar, A., Soga, K., and Mair, R. J. (2005); "Estimating the effects of tunneling on existing pipelines," *ASCE Journal of Geotechnical and Geonvironmental Engineering,* 131(11), 1399-1410.

Zymnis, D. M., Whittle, A. J., and Chatzigiannellis, Y. (2011); "Effect of cross-anisotropy on ground deformations caused by tunneling for Jubilee Line Extension below St. James's Park," submitted to Géotechnique.

Project	Source	Construction Method	Face Conditions	R (m)	H (m)	Method	Input parameters			
							ν or [α]	u_ε (mm)	$\Delta V_L/V_0$ (%)	ρ
N-2 San Francisco: Line #4	Clough et al., 1983	EPB	Soft Clay	1.85	9.7	3-point	0.5	-17.9	2.0	1.76
						LSS*	0.5	-16.0	1.8	2.11
N-2 San Francisco: Line #2						3-point	0.5	-64.4	7.2	0.43
						LSS*	0.5	-56.0	6.3	0.61
Mexico City Sewer	Romo, 1997	Slurry shield	Soft Clay	2.00	12.8	3-point	0.12	-22.0	2.2	1.53
						LSS*	0.5	-25.0	2.5	1.34
Madrid Metro Extension: Line 1 Sect. 7	Sagaseta & Gonzalez, 1999	Open Face (Belgian)	V. Stiff Clay	4.44[1]	15.2	3-point	0.5	-13.5	0.6	0.22
						LSS*	0.5	-14.0	0.6	0.21
						S&G	0.5	-17.0	0.8	0.20
Second Heinenoord	E. P. van Jaarsveld et al., 1999	Slurry shield	Dense Sand	4.15	16.7	LSS*	[1.09]	-26.0	1.3	0.80
Heathrow Express Trial Tunnel (Type 3)	Deane & Bassett, 1995	Open Face NATM	V. Stiff Clay	4.25[2]	19.0	3-point	0.5	-46.7	2.20	0.26
						LSS*	0.5	-32.0	1.51	0.62

Notes:

1. Equivalent radius: Horseshoe-shaped section
2. Equivalent radius: NATM section

Table 1: Summary of case studies

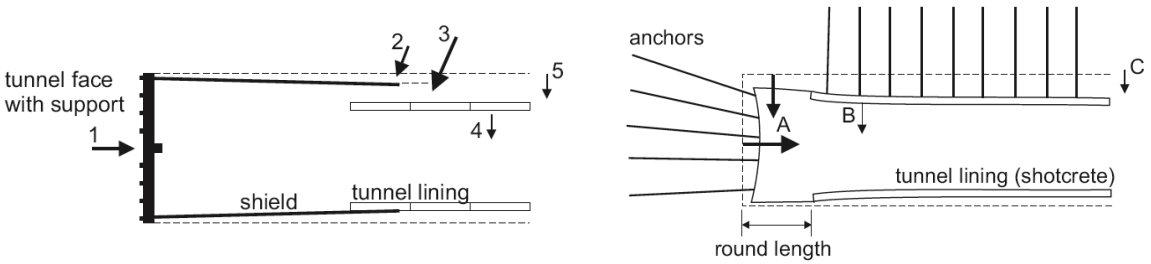

1. Stress relief at tunnel face
2. Shield over-cut & ploughing
3. Tail Void
4. Deformation of lining
5. Consolidation of soil

a) Closed-face tunnel

A. Deformation at tunnel heading
B. Deformation of lining
C. Consolidation of soil

b) Sequential excavation

Figure 1: Sources of ground movements associated with tunneling (after Möller, 2006)

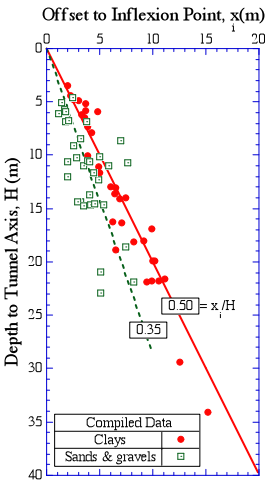

a) Width of surface settlement troughs

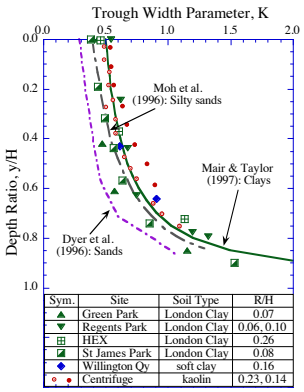

b) Width of sub-surface settlement troughs

Figure 2: Empirical estimation of inflexion point (after Mair & Taylor, 1997)

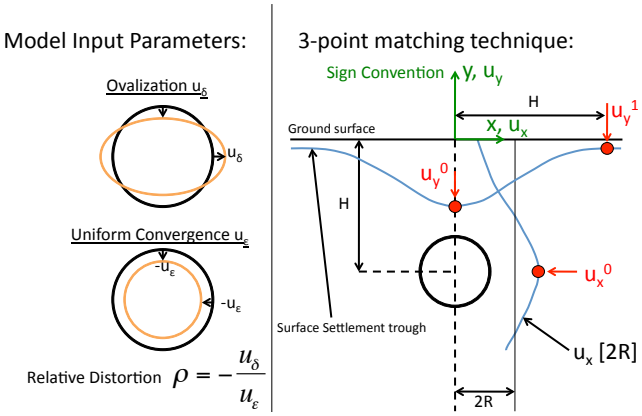

Figure 3: Sign convention and reference parameters for three-point matching method

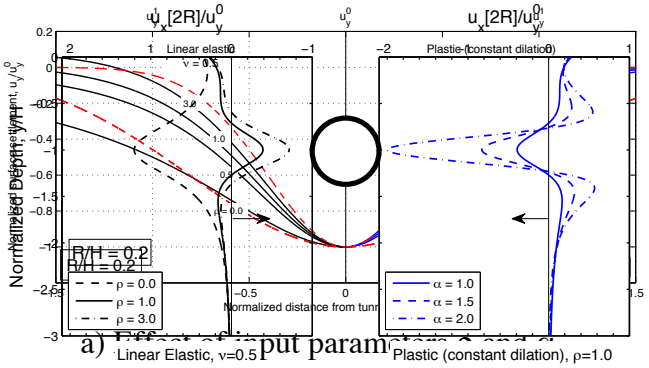

a) Effect of input parameters ρ and α on shape of surface settlement trough

b) Effect of parameters ρ and α on lateral displacements at offset, x/2R = 1

Figure 4: Typical analytical predictions of surface settlements and subsurface lateral dispacements

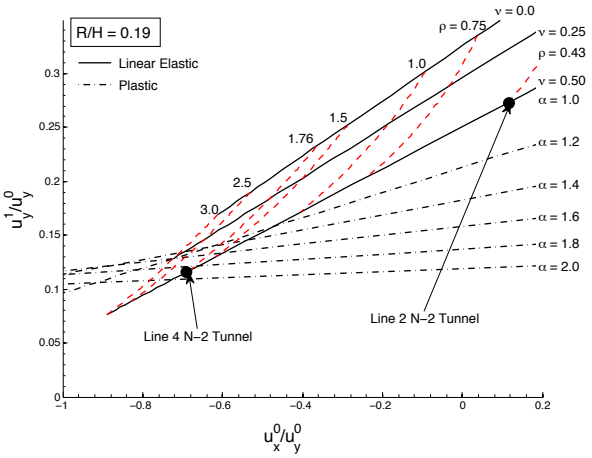

a) Determination of ρ, ν or α

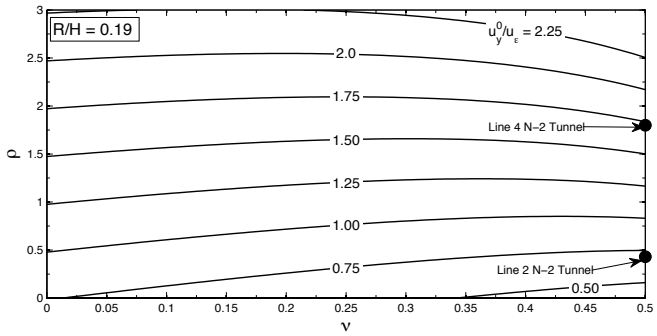

b) Determination of u_ε

Figure 5: Illustration of 3-point measurement procedure for estimating input parameters

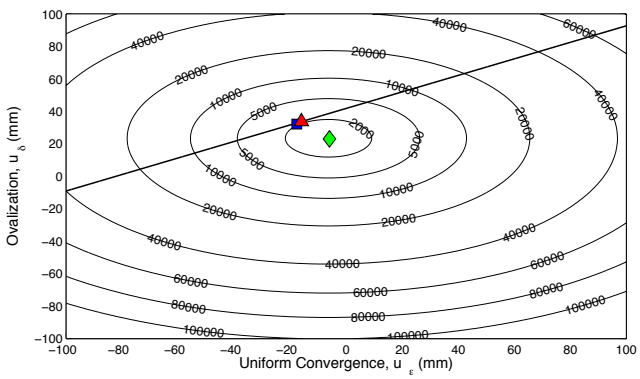

EPB Tunnel, N-2 San Francisco; Line #4						
Symbol	Method	Fit	$\Delta V_L / V_0$ (%)	u_ε (mm)	ρ	ν
■	3-point fit	Analytical	2.0	-17.6	1.82	0.5
▲	LSS*	Analytical	1.8	-16.0	2.11	0.5
◆	LSS	Analytical	0.7	-6.0	3.83	0.5
	Square Solution Error (mm^2) from 28 points, Avg error = 1.7mm					
	Centerline Surface Settlement Fit					

a) N-2: Line #4

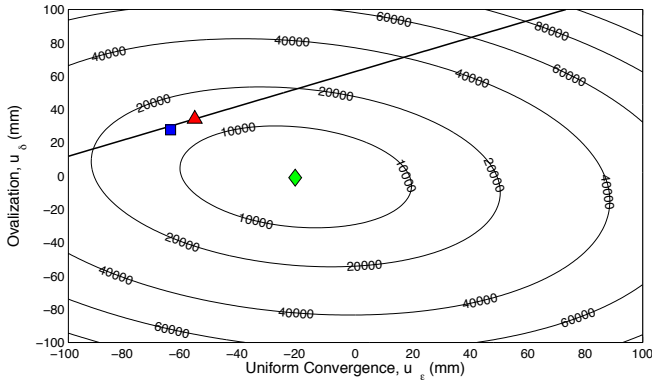

EPB Tunnel, N-2 San Francisco; Line #2						
Symbol	Method	Fit	$\Delta V_L / V_0$ (%)	u_ε (mm)	ρ	ν
■	3-point fit	Analytical	7.2	-64.4	0.43	0.5
▲	LSS*	Analytical	6.3	-56.0	0.61	0.5
	LSS	Analytical	2.4	-21.0	-21.0	0.5
	Square Solution Error (mm^2) from 20 points					
	Centerline Surface Settlement Fit					

b) N-2: Line #2

Figure 6: Illustration of least squares procedures for input parameter selection using N-2 Case Study, San Francisco

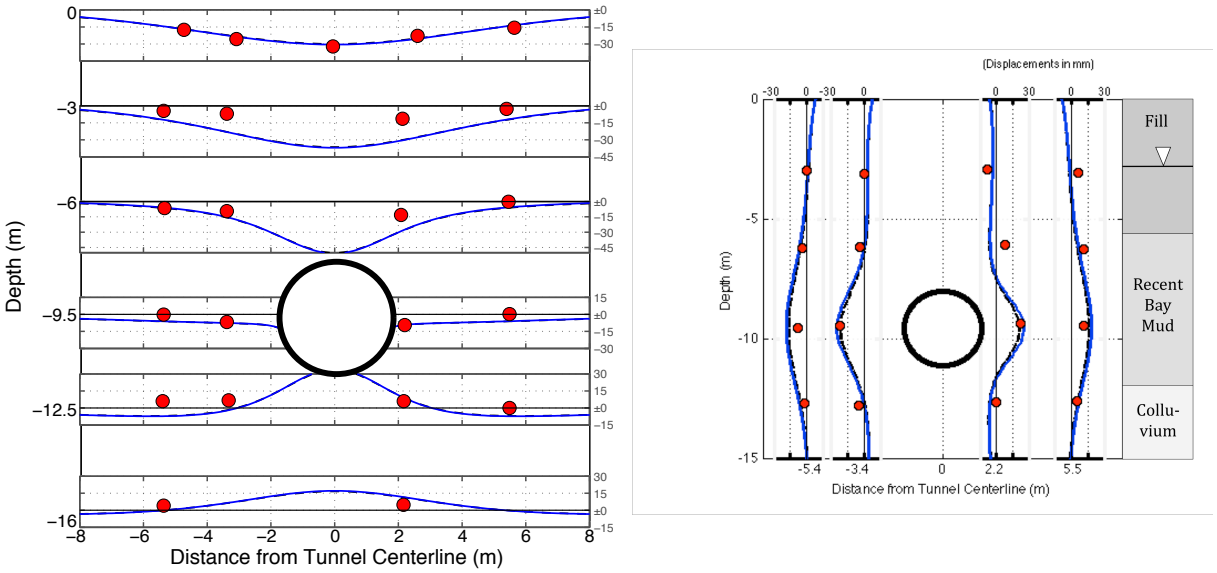

a) Vertical displacements b) Lateral displacements

EPB Tunnel, N-2 San Francisco; Line 4						
Line	Method	Fit	$\Delta V_L / V_0$ (%)	u_ε (mm)	ρ	ν
– – – –	Analytical	3-point	2.0	-17.6	1.82	0.5
———	Analytical	LSS* (28 points)	1.8	-16.0	2.11	0.5

Figure 7: Computed and measured displacements for N-2 Tunnel, San Francisco; Line 4

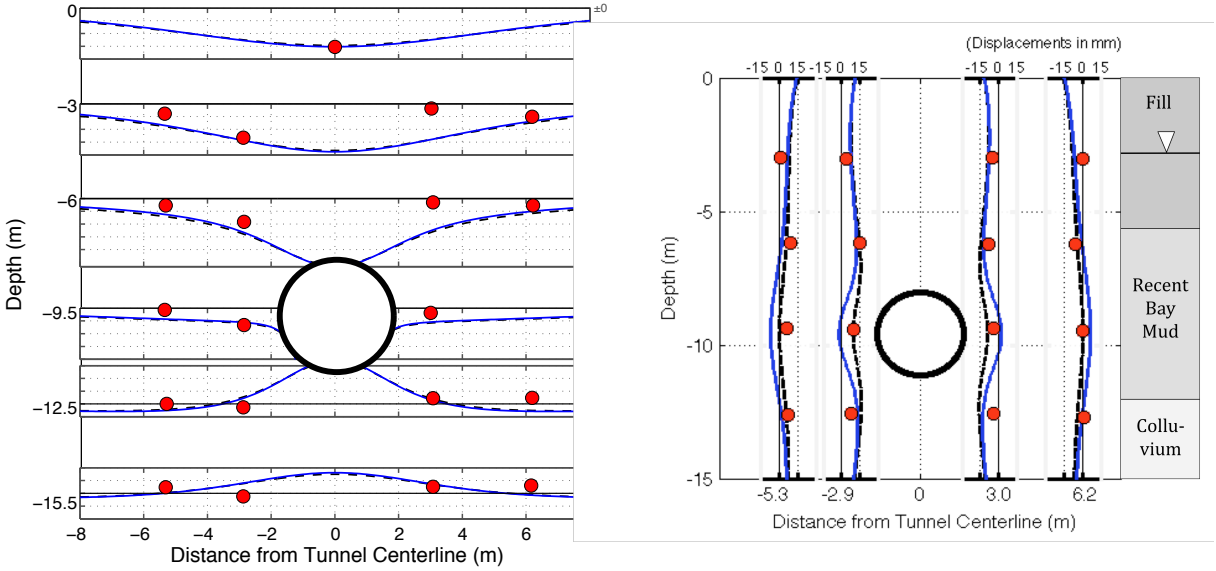

a) Vertical displacements b) Lateral displacements

EPB Tunnel, N-2 San Francisco; Line 2						
Line	Method	Fit	$\Delta V_L / V_0$ (%)	u_ε (mm)	ρ	ν
– – – –	Analytical	3-point	7.2	64.4	0.43	0.5
———	Analytical	LSS* (20 points)	6.3	-56.0	0.61	0.5

Figure 8: Computed and measured displacements N-2 Tunnel, San Francisco; Line 2

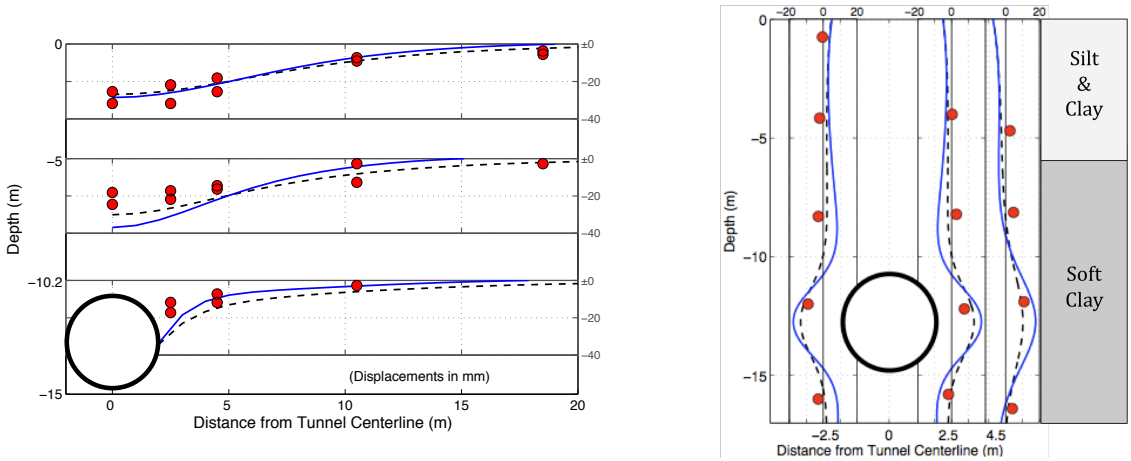

a) Vertical displacements b) Lateral displacements

EPB Tunnel, Sewer tunnel Mexico City						
Line	Method	Fit	$\Delta V_L / V_0$ (%)	u_ε (mm)	ρ	ν
– – – –	Analytical	3-point	2.2	-22	1.53	0.12
———	Analytical	LSS* (26 points)	2.5	-25	1.34	0.5

Figure 9: Computed and measured displacements for EPB Sewer Tunnel, Mexico City

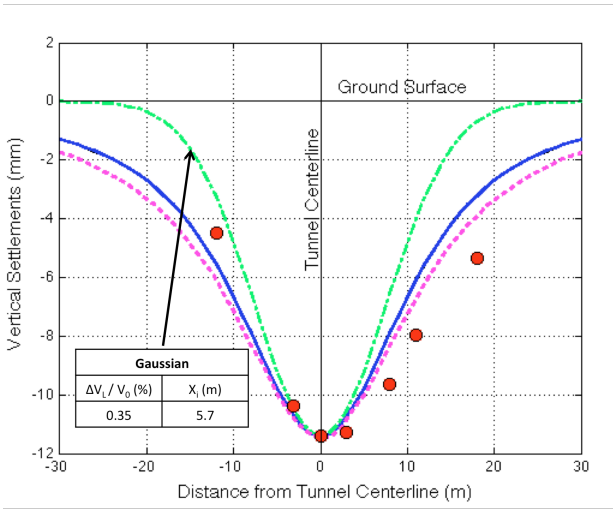

a) Surface Settlements

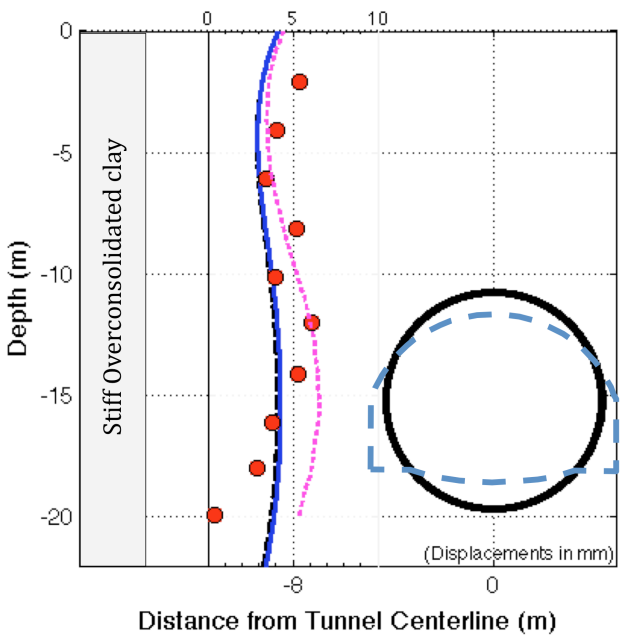

b) Lateral Displacements

Open face tunnel, Madrid Metro Extension						
Line	Method	Fit	$\Delta V_L / V_0$ (%)	u_ε (mm)	ρ	ν
– – – –	Analytical	3-point	0.6	-13.5	0.22	0.5
———	Analytical	LSS* (17 points)	0.6	-14.0	0.21	0.5
– – – –	Analytical (Gonzalez & Sagaseta, 1999)	3-point	0.8	-17.0	0.20	0.5

Figure 10: Computed and measured displacements for Madrid Metro Extension Tunnel Line 1; Section 7

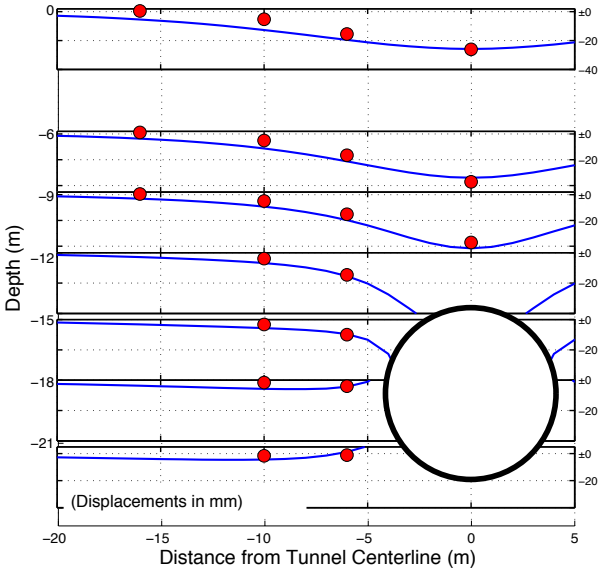

a) Vertical displacements

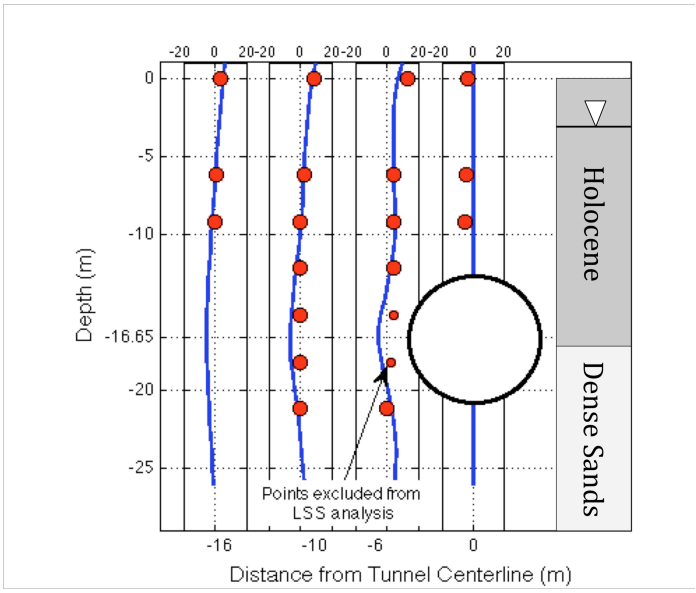

b) Lateral Displacements

Shield driven slurry tunnel, Second Heinenoord Tunnel						
Line	Method	Fit	$\Delta V_L / V_0$ (%)	u_ε (mm)	ρ	α
———	Analytical	LSS* (38 points)	1.3	-26	0.80	1.09

Figure 11: Computed and measured displacements for Second Heinenoord Tunnel

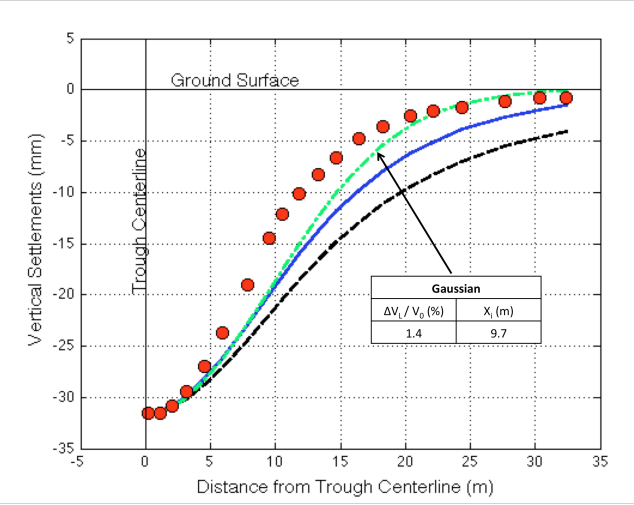

a) Surface Settlements

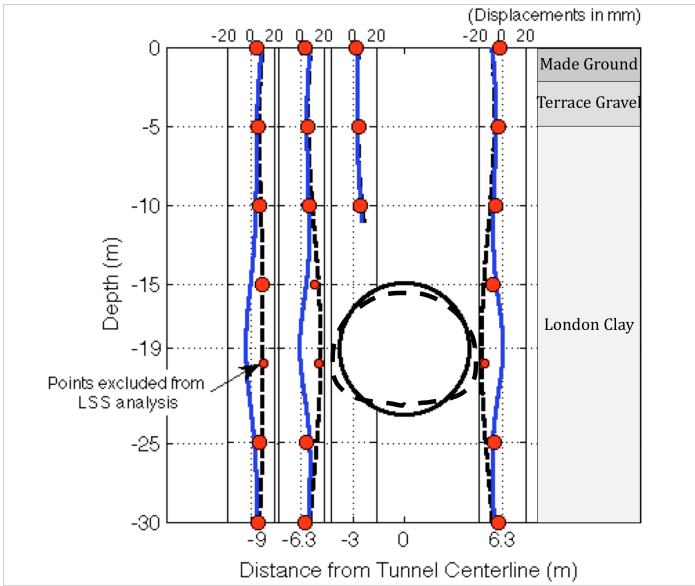

b) Subsurface Lateral Displacements

NATM Heathrow Express Trial Tunnel (Type 3)						
Line	Method	Fit	$\Delta V_L / V_0$ (%)	u_ε (mm)	ρ	ν
– – – –	Analytical	3-point	2.2	-46.7	0.26	0.5
———	Analytical	LSS* (40 points)	1.5	-32.0	0.62	0.5

Figure 12: Computed and measured displacements for NATM Heathrow Express Trial Tunnel